Journal of Visualization, Vol. 6, No. 3 (2003) 263-272

A New Super-Resolution PIV Accelerated by Characteristic Pixel Selection

Yamamoto, Y.* and Uemura, T.*

* Department of Systems Management Engineering, Kansai University, Yamate-cho 3-3-35, Suita, Osaka, 564-8680, Japan.
E-mail: yamayasu@iecs.kansai-u.ac.jp

Received 21 October 2002
Revised 11 March 2003

Abstract : A new high-speed super-resolution PIV was proposed using characteristic pixel selection to accelerate the successive abandonment (SA) with recursive window subdivision. The performance and applicability of the proposed PIV were evaluated. In the SA calculation with the characteristic pixel selection, 1000 candidates are narrowed down to only one at over 50 % of the measurement points, and the number of error vectors is reduced because the difference between the cumulative intensities of a correct candidate and of other ones becomes clear due to the characteristics of selected pixels. In all recursive processes, error checks are carefully performed using the summation of the distribution of the cumulative intensity difference distribution, which is suitable for the SA method. In a comparison of the time per velocity vector, the present super-resolution PIV was shown to be 10 times faster than the former ordinary resolution PIV. Another feature of the present super-resolution PIV is that the velocity vectors are obtained in the region very close to the image boundaries and masked regions by using the recursive algorithm.

Keywords : Super-resolution PIV, Successive abandonment method, Characteristic pixel selection, Boundary region, Mask

1. Introduction

Particle image velocimetry (PIV) is a powerful tool for measurement of the spatio-temporal distribution of fluid velocity. Recently, as the development of photographic tools such as cameras, illuminations, and so on, high-density particle images can be obtained. Along with such developments, some algorithms of super-resolution PIV have been proposed (Kean et al. 1995; Hart 2000a; Stitou & Riethmuller 2001). In particular, Hart's algorithm, in which interrogation windows are recursively subdivided, is a useful technique that involves a simple algorithm and allows a higher resolution while carefully removing erroneous vectors. However, recursive calculation using the ordinary cross-correlation method requires too much computational time. In order to reduce it, Hart proposed an image compression technique. However, that technique requires complex computational procedures. In this paper, we propose a new algorithm using not image compression but characteristic pixel selection in order to accelerate the super-resolution PIV with recursive

window subdivision.

The proposed PIV algorithm is developed based on the successive abandonment (SA) method (Kaga et al. 1993). In the former SA method, which calculates cumulative intensity differences line by line in an interrogation window, calculation speed depends on the intensity pattern in the interrogation windows, while non-effective abandonment leads to the occurrence of error vectors. In the present paper, we introduce a new process into the SA method. This new process consists of the selection of two characteristic pixels from each line in an interrogation area, and preprocessing the candidates using the characteristic pixels. The characteristic pixels can be such pixels as that with the highest brightness, and the one with the lowest. By means of this processing method, similarity between two pictures can be defined distinctively and consequently the SA method can be accelerated.

For recursive PIV, an error check is needed in order that displacement of smaller windows are not affected badly by ones of larger windows. Hart (2000b) proposed an error check method using multiplication between correlation distributions of overlapped neighboring interrogation windows. The present algorithm is based on the cumulative difference of intensity, not cross-correlation, so we modified the Hart's error check method in order to make it suitable for SA.

Another feature of our PIV is that the velocity vectors are obtained in the region very close to the boundary of images and masked regions, in which large interrogation windows hinder the calculation of displacements. In the present study, velocity vectors in that region are obtained by applying the recursive approach. Through the application of many improvements, a new algorithm of very high-speed super-resolution PIV was developed.

2. Calculation Method

2.1 Outline

Our super-resolution PIV is composed of pattern matching, error detection, sub-pixel displacement calculation, and the treatment of the boundary region. A flow chart of the present PIV is shown in Fig. 1. At first, candidates are narrowed down by SA calculation using selected pixels. At the measurement points where candidates are not sufficiently abandoned, SA is applied line by line. Displacements are then determined through the error check algorithm. Following these procedures, interrogation windows are divided into half size (n/2 x n/2 pixels) and the same procedures are performed recursively. However, the search windows are limited to the region near the displacements calculated by the previous level with larger interrogation windows. The cumulative difference is calculated only by selected pixels except for the final level, because displacements can be detected without errors by the selected pixels in the small-size search windows. By repeating these procedures recursively, resolution is increased while using less computational effort and producing fewer errors. At the final level, all pixels in the interrogation window are used to determine the displacement because the final level calculation is directly concerned with accuracy and the time spent for calculation of small-size interrogation windows is short. After the final level calculation, sub-pixel accuracy displacements are calculated by means of parabolic interpolation around the peak of cumulative difference distribution. In this section, each part will be explained.

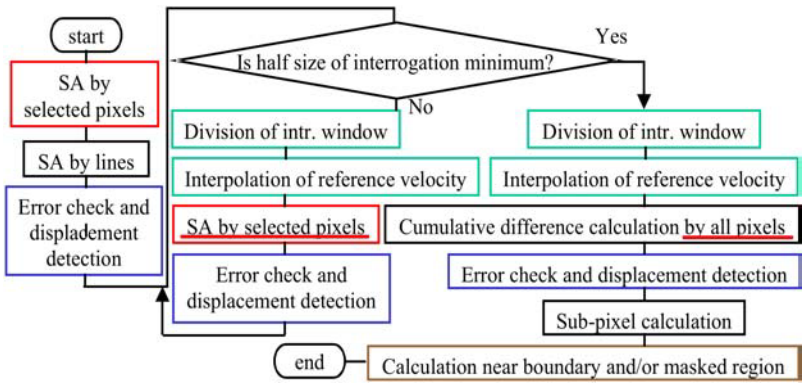

Fig. 1. Flow chart of the present super-resolution PIV.

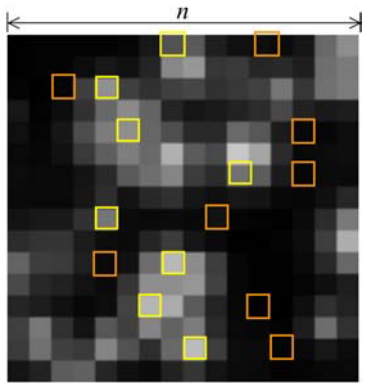

Fig. 2. A sample of selected characteristic pixels.

2.2 Pattern Matching and its Acceleration

As a template matching method, the successive abandonment (SA) method proposed by Kaga et al. (1993) is used. The SA method uses cumulative intensity difference D as the matching index,

$$D(i,j)=\sum_{l=-n/2}^{n/2}\sum_{m=-n/2}^{n/2}\left|f(i+l,j+m)-g(l,m)\right|=D_{part}(i,j,k)+\sum_{l=k+1}^{n/2}\sum_{m=-n/2}^{n/2}\left|f(i+l,j+m)-g(l,m)\right| \quad (1)$$

where g is the intensity of a template image and f is the image intensity of the next frame. When D is minimum, the point (i, j) is considered as the destination of the template image. Here, in the case that the candidate pattern is largely different from the template pattern, D of equation (1) becomes a large value before finishing the calculation of all summation. So, in the SA method, cumulative difference is calculated line by line, and the candidates whose D_{part} becomes larger than threshold are then abandoned. The threshold is determined by $\beta D_{part,minimum}$. β can be determined by the F-test because distribution of D obeys a one-sided normal distribution, as is verified by Kaga et al. (1993). So, β is calculated by,

$$\beta=\sqrt{F_{kn-1}(\gamma)} \quad (2)$$

where, $F_{kn\text{-}1}(\gamma)$ is the F-value corresponding to the level of significance γ and the degrees of freedom kn-1.

In the previous SA method, which calculates cumulative intensity difference per line in an interrogation window, calculation speed depends on the intensity pattern in the interrogation windows and non-effective abandonment leads to the occurrence of error vectors. So, we introduce a new algorithm using selected characteristic pixels in order to make the difference between correct candidate and others clear in the early stage of SA. As characteristic pixels, we choose the highest intensity pixels and the lowest ones in every two lines of the interrogation windows as shown in Fig. 2. When the size of a interrogation window is set to n x n pixels, the number of selected pixels is n. Candidates are narrowed down by calculation of the cumulative difference of intensity for these selected pixels.

Figure 3 shows sample distributions of the cumulative intensity difference. Fig. 3(*a*) shows the case by using n pixels of centerline of interrogation window and Fig. 3(*b*) shows that by selected n characteristic pixels, where n=32. Images used in this sample are the PIV standard images #01 provided by the Visualization Society of Japan (Okamoto et al. 2000). It is found that the selected pixel approach strongly clarifies the peak of cumulative intensity difference, while the distribution by centerline pixels does not show such a distinct peak even though the number of calculated pixels is

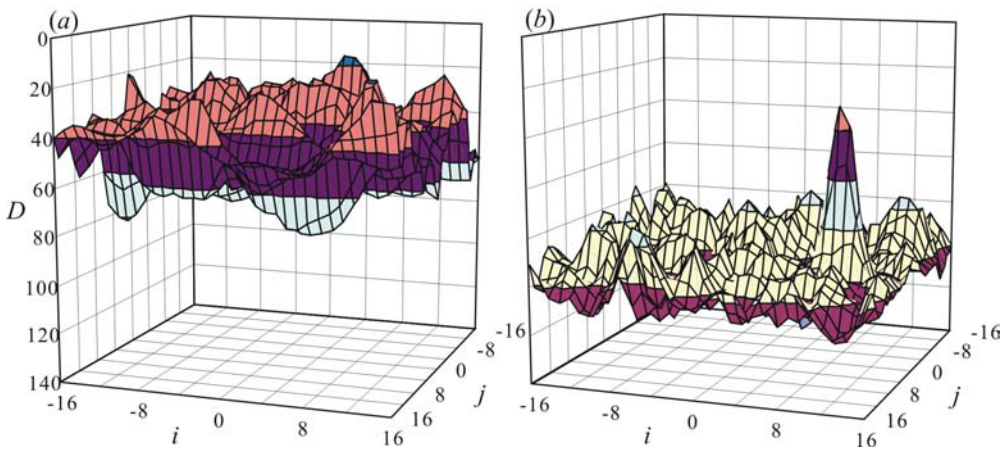

Fig. 3. Distribution of cumulative differences of intensity (the direction of vertical axes is opposite). (a) using n pixels of the centerline of the interrogation window, (b) selected n characteristic pixels. n=32.

the same. Depending on the templates, centerline pixels cannot represent the template pattern. However, even if we can choose the best representative line, that is only very local characteristics. And we do not know the way to select the most characteristic lines. So our method selects not line but pixels from all pixels of the template window. As the result of abandonment for this sample distribution, the number of residual candidates is 97 for (*a*) and 4 for (*b*). Thus, calculation using only *n* selected pixels can determine the approximate displacement in this sample case. For more detailed comparison of the selected-pixel calculation with the centerline one, Table 1 shows the rate of the number of measurement points for the number of candidates not abandoned. At over 50% of the measurement points, the candidates are narrowed down to less than 1% (the size of the search window is 33 x 33, thus the number of total candidates is 1089).

At the residual measurement points where the candidates are not narrowed down by selected pixels, the cumulative differences of one line are calculated and candidates are abandoned after calculation line by line. In this calculation, a line which contains the highest intensity pixel is selected out of lines not yet calculated. SA calculation is stopped when candidates are narrowed down to less than 1%, because error check can detect the displacements, as explained later. Table 2 shows the rate of measurement points whose candidates are narrowed down to less than 1% for the number of calculated lines. It is found that at 99% of measurement points, the present algorithm can narrow the candidates down to 1% by 1/4 calculation of interrogation window (the size of interrogation window is 32 x 32 in this sample). However, calculation of the half of the interrogation windows without the use of pixel-selection cannot narrow down the candidates at about 40 % of the measurement points. This improvement clearly demonstrates the features of the proposed algorithm.

Table 1. The rate of measurement points for the number of candidates not abandoned.

The number of candidates not abandoned	rate of measurement points [%]	
	centerline	selected pixels
1~10	32.5	55.7
11~500	63.8	39.2
500~1089	3.7	5.1

Table 2. The rate of measurement points whose candidates are narrowed to less than 1% for the number of calculated lines.

The number of calculated lines	rate of measurement points [%]	
	without pixel selection	with pixel selection
selected pixels		55.7
1~4	35.2	38.5
5~8	11.7	4.6
9~16	14.0	0.9
17~24	5.3	0.1
25~32	33.8	0.1

2.3 Error Check and Displacement Determination

After the candidates are narrowed down at all the measurement points, error check is applied. Interrogation windows are set to overlap with neighboring ones in their half-region. When displacements are calculated by using overlapping interrogation windows, the minimum value of the cumulative intensity difference of the neighboring points is obtained in the similar position. So the summation of cumulative intensity difference distribution emphasizes the correct minimum value and weakens the wrong ones relatively as shown in Fig. 4. Here, D at the abandoned candidate is set to the threshold value so as not to interfere with the summation. The position of the local minimum value of the cumulative intensity difference nearest to the position of the minimum value of the summed one is determined as the displacement. Unlike Hart's algorithm (Hart 2000a) which uses the product of correlation distribution, we use summation. This we consider more effective because there is a possibility that neighborhoods of correct peaks are abandoned. Through this error elimination procedure, displacements from a few candidates can be determined, and thus the SA does not have to narrow candidates to only one.

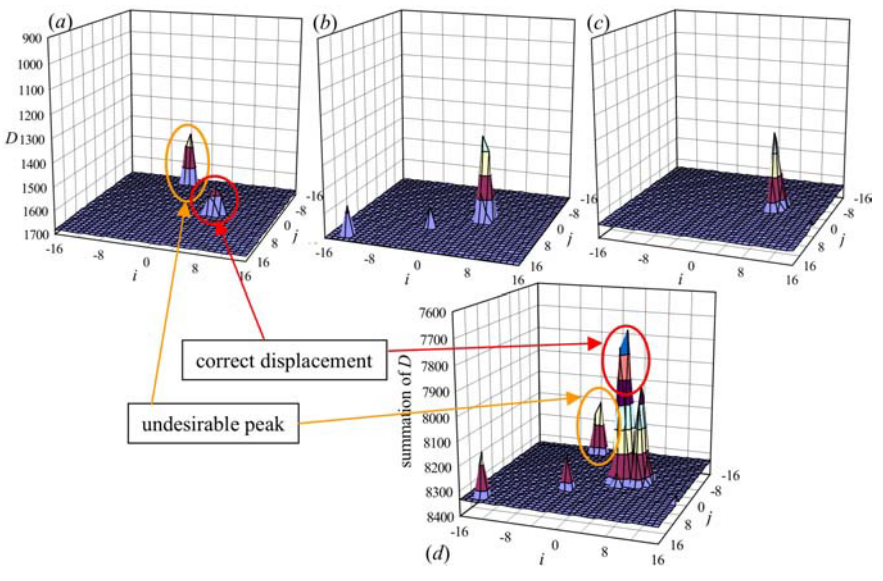

Fig. 4. Effect of summation of cumulative difference distribution (the direction of vertical axes is opposite). (a) cumulative difference distribution at a reference point, (b)& (c) those of neighboring points, (d) summation of (a) and all neighboring distributions including (b)&(c). (flat planes correspond to the points of abandoned candidates).

2.4 Treatment of Boundary and/or Masked Regions

Large interrogation windows hinder the calculation of displacements near the image boundaries as shown in Fig. 5. The nearest point to the boundary where the velocity vector can be calculated is decided by half of interrogation window size plus the search window size. Outside of these points, pattern matching cannot be done. In this study, velocity vectors in that region are obtained by applying the following approach (see also Fig. 6). At first, the inner region is calculated until the last level, as mentioned in the above section. In one layer of measurement points nearest to the inner region, displacements are predicted by linear extrapolation. Using these reference displacements, candidates are calculated using last-level interrogation windows and small-size search windows. The correct displacements are obtained by means of the aforementioned error elimination method. The same procedures are repeated from the inner region to the boundary, line by line. Of course, this calculation is not performed when a search window determined on the basis of predicted displacement includes the outer points of the image.

In actual measurements, there are cases in which some objects are included in PIV images. In such cases, mask treatments are often applied. In a mask treatment, only painting in black in the object region causes error vectors. In our PIV, mask regions are treated in the same way as boundary regions are. At first, interrogation windows and search windows are checked as to whether these windows include the mask region. At these windows that include the mask region, velocity is not calculated until the last level calculation. After the final level calculation at other points, velocities in these regions are calculated using the same approach as that used in the boundary region.

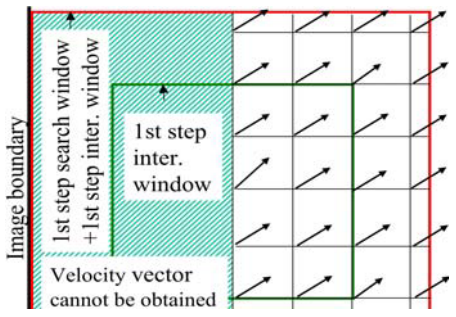

Fig. 5. Blank in the boundary region.

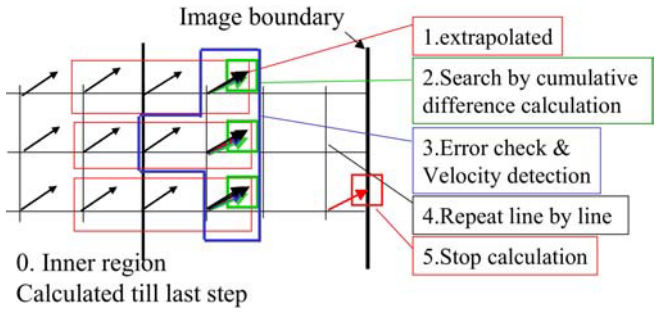

Fig. 6. Treatment of boundary and/or masked region.

3. Results and Discussion

Figure 7 shows the results obtained by the present super-resolution PIV with and without boundary calculation for standard image #04. The sizes of the interrogation windows are 32 x 32 pixels at level 0 and 4 x 4 pixels at the last level, and the sizes of the search windows are 35 x 35 pixels at level 0 and 7 x 7 at other levels. It is found that very high-density velocity vectors can be obtained using our PIV. Without the boundary calculation shown in Fig. 7(*a*), the outside of the image is ineffective (the region of over 32/2 + 35/2 = 34 pixel width is blank). On the other hand, using the boundary calculation shown in Fig. 7(*b*), velocity vectors are obtained effectively within the boundary limit; *i.e.*, 2 pixels next to the boundary in the upper stream and the outflow limit in the down stream and the error vectors caused by out-of-image motion are not calculated. It is found that the present PIV can obtain smooth velocity distribution as shown in Fig. 7(*c*), which is an expanded image of an enclosed region of (*b*).

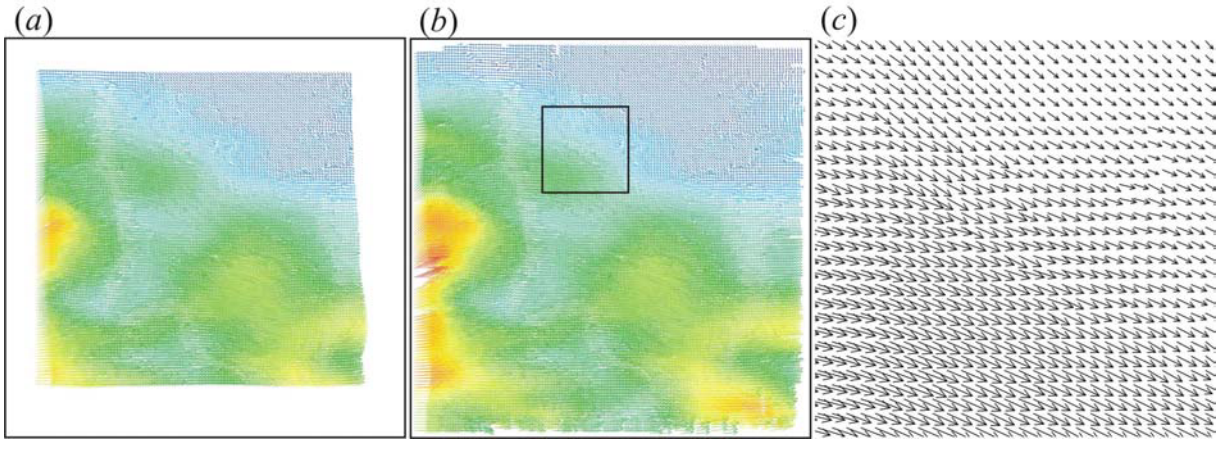

Fig. 7. Results of super-resolution PIV for VSJ standard image PIV #04. (image size 256x256, interrogation sizes are 32x32 pixels at level 0 and 4x4 pixels at the last level; search sizes are 35x35 pixels at level 0 and 7x7 at other levels). (a) without boundary calculation, (b) with boundary calculation, (c) partially expanded image of enclosed region of (b).

In regard to measurement accuracy, measured velocity data are compared to the attached data of PIV standard images. Reference data at all measurement points are obtained by bi-linear interpolation and extrapolation of the original data. Figure 8 shows the scatter plot of the deviation of measured velocity from reference velocity, where the unit of velocity is pixels/frame. The number of plots is 15534. It is found that almost all erros are within 0.5 pixels/frame. Thus, the mean value of absolute error is 0.29 pixels/frame and the root mean square of error is 0.40 pixels/frame. Further discussion about accuracy is in later.

Table 3 shows the time spent to calculate the velocity vectors at each level and the total time. It is shown that the selected pixel approach decreases the calculation time to about 70% of that of the former SA method. The former ordinary-resolution PIV takes 656ms/625vectors = 1.05ms/vector. So, the time per velocity vector by our super-resolution PIV is about 10% of the conventional resolution PIV. A Pentium III 933MHz computer was used in this study.

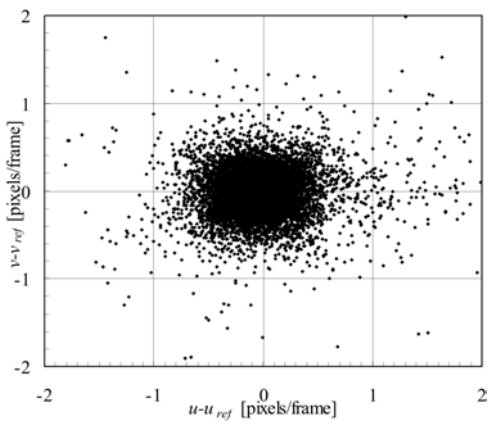

Fig. 8. Deviation of measured velocity from reference velocity.

Table 3. Computational time.

	without pixel selection	with pixel selection
level 0 [ms]	282	219
level 1 [ms]	375	47
level 2 [ms]	515	172
level 3 [ms]	953	953
boundary [ms]	391	391
total [ms]	2516	1782
the number of vectors [-]	15534	15534
time/vector [ms]	0.162	0.115

Figure 9 shows the effect of mask treatment for PIV standard images #04 partially painted in black. Figure 9(*a*) is the original image. Figure 9(*b*) shows the result without special treatment. Fig. 9(*c*) shows the result obtained by the present approach. Many error vectors are calculated without special treatment. On the other hand, the present approach can obtain as many velocity vectors as possible in the region where the reasonable velocities can be obtained, *i.e.*, to the inflow limit in the upper stream and just next to the mask boundary in the down stream. The number of velocity vectors obtained by special treatment is 665. The number of velocity vectors different from the results shown in Fig. 7 is only 4 vectors. These results show that our approach is very effective for mask treatment.

A sample result for real images is shown in Fig. 10. This case shows the treatment of a flow around a flat plate. In the general recursive algorithm of super-resolution PIV, such a flow cannot be treated, because the flow direction is the opposite on both sides of the plate. In our measurement, the region of the plate is treated as a masked region. It is found that the present PIV obtains smooth velocity distributions in the region very close to the plate.

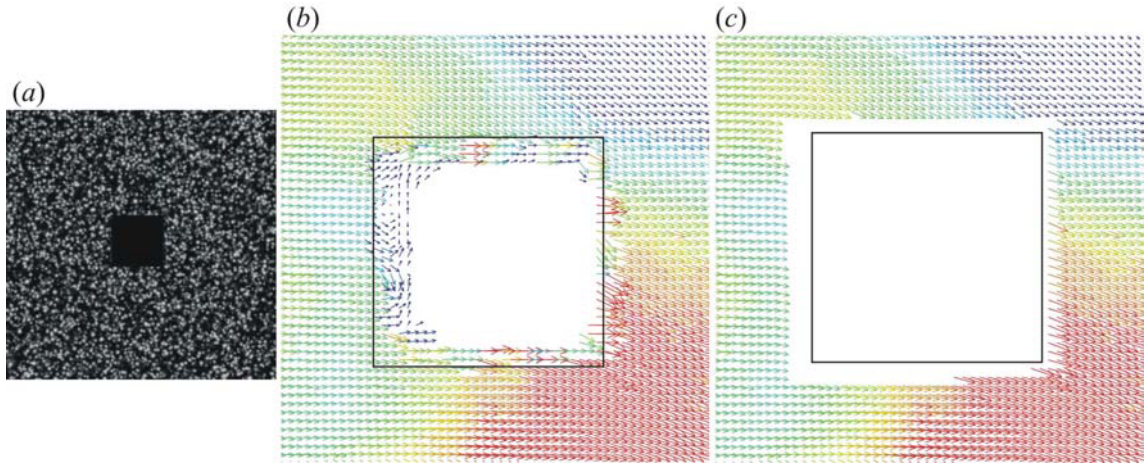

Fig. 9. Effect of mask treatment. (a) tested image (PIV standard image #04) whose center region is painted black (b) without mask treatment (c) with mask treatment. (b) & (c) are partially expanded in the region near the black-painted one.

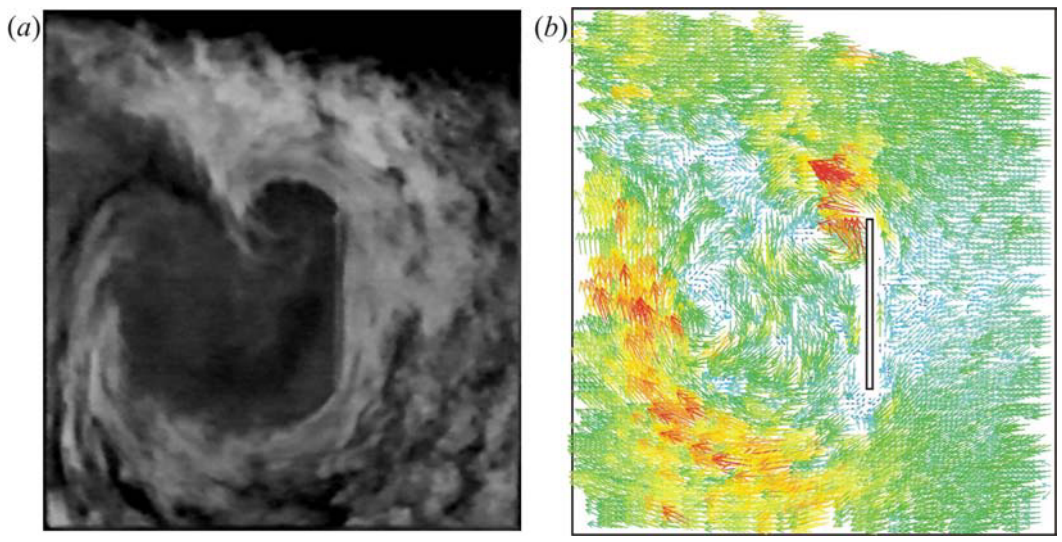

Fig. 10. Result for a real image. (a) tested image, (b) velocity vectors obtained by the present SR-PIV.

For further discussion regarding this method's accuracy, the results of another test case are shown in Fig. 11. Figure 11 (*a*) shows the tested synthetic image (256x256 image size, mean particle diameter: 4 pixels, the number of particles in the image: about 10000) which is made by following the PIV standard image. Horizontal velocity has a linear profile from 0 to 6.4 pixels/frame along the vertical axis, so the shear rate is 6.4/256=0.025 /frame. The size of the interrogation window and mean particle diameter is 4 pixels, so the difference of velocity at 4 pixels is 0.1 pixels/frame. The results shown in Fig. 11(*b*), which shows the vertical distribution of the horizontal velocity component, reveal the tendency of peak locking. The measurement deviation from correct velocity is shown in Fig. 11(*c*). It is found that almost all the deviations are within about 0.5 pixels/frame regardless of the 0.1 pixels/frame velocity differences due to linear shear. This result shows that the sub-pixel calculation needs to be improved. At the boundaries, it is found that the velocity vectors obtained by the present treatment of boundaries are reasonable. (The size of the boundary region in this sample is 25 pixels). A case of parabolic velocity distribution is also tested (the result is omitted in this paper). We found that accuracy does not depend on the velocity gradient, and that almost all the deviations are within approximately 0.5 pixels/frame as in the results shown in Fig. 11.

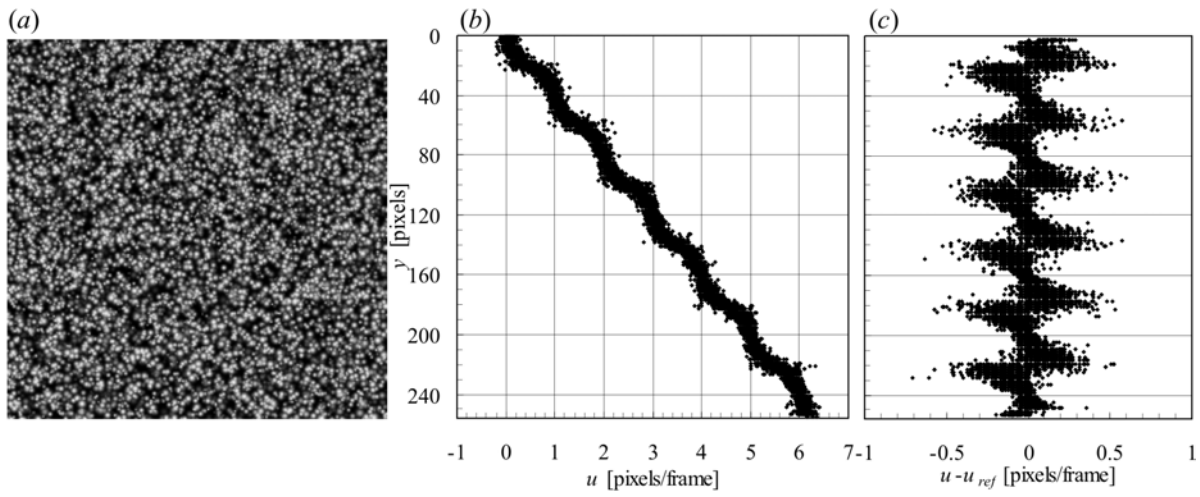

Fig. 11. Results for linear shear flow. (a) tested image, (b) vertical distribution of horizontal velocity component, (c) deviation from correct velocity. (The size of the interrogation window is 4x4 pixels.)

4. Conclusion

A new algorithm for recursive super-resolution PIV was introduced. Pattern matching based on the successive abandonment (SA) method was accelerated by the characteristic pixel selection approach. The error check of Hart's algorithm was modified to be suitable for the SA method, and a treatment of the boundaries and masks was proposed. The availability of our super-resolution PIV was examined by using synthetic images and real images. As a result, the following points were revealed. The proposed super-resolution PIV is 10 times faster than former ordinary-resolution PIV due to the large effect of the selected pixel approach. The level of accuracy is fairy high. This method can obtain velocity vectors effectively in the region near the boundaries and masks.

It is necessary to continue examining the present method's range of application and accuracy. In particular, sub-pixel accuracy needs to be improved. For example, the gradient method described by Sugii et al. (2000) can be combined with the present PIV algorithm because the gradient method does not depend on pixel-accuracy displacement detection. We will explore this combination in our

future research.

Acknoweldgements

The authors are grateful to Messrs. M. Nishida and S. Kadota for their assistance with software programming.

References

Hart, D. P., Super-resolution PIV by Recursive Local-correlation, J. Flow Visualization, 3-2 (2000a), 187-194.
Hart, D. P., PIV error correction, Exp. in Fluids, 29-1 (2000b), 13-22.
Kaga, A., Inoue, Y. and Yamaguchi, K. Pattern Tracking Algorithms using Successive Abandonment, J. Flow Visualization and Image Processing, 1-4 (1993), 283-296.
Kean, R. D., Adrian, R. J. and Zhang, Y., Super-resolution Particle Imaging Velocimetry, Meas. Sci. Technol., 6 (1995), 754-768.
Okamoto, K. Nishio, S., Saga, T. and Kobayashi, T., Standard Images for Particle-image Velocimetry, Meas. Sci. Technol., 11 (2000), 685-691.
Stitou, A and Riethmuller, M. L., Extension of PIV to Super Resolution using PTV, Meas. Sci. Technol., 12 (2001), 1398-1403.
Sugii, Y., Nishio, S., Okuno, T. and Okamoto, K. A Highly Accurate Iterative PIV Technique using a Gradient Method, Meas. Sci. Technol., 11 (2000), 1666-1673.

Author Profile

Yasufumi Yamamoto: He is a research associate of the Department of Systems Management Engineering at Kansai University, Japan. He received his Doctoral degree in Mechanical Engineering from Osaka University in 1999. He worked as a postdoctoral fellow researcher in the Civil Engineering Department at Ritsumeikan University from 1999 to 2000. His research interests are numerical and experimental analyses of multiphase flow systems.

Tomomasa Uemura: He graduated from the Department of Mechanical Engineering, Osaka University, in 1965, and received his Doctoral degree in 1978 from Osaka University while working as a research associate. He moved to his current position at Kansai University in 1993. He has developed optical techniques for flow visualization techniques including LDV, PIV, and PTV. His current research interests are directed at flows influenced by surface tension, and micro-flows. He is also interested in applications of image processing techniques for detecting and pursuing temporal changes in bio- and environmental phenomena.